Fast-Ion Energy-Flux Enhancement from Ultrathin Foils Irradiated by Intense and High-Contrast Short Laser Pulses

A. Andreev,[1] A. Lévy,[2] T. Ceccotti,[2] C. Thaury,[2] K. Platonov,[1] R. A. Loch,[3] and Ph. Martin[2,1]

[1]*STC Vavilov State Optical Institute, 12 Birzhevaya line, 199034 St. Petersburg, Russia*

[2]*CEA, IRAMIS, SPAM, F-91191 Gif-sur-Yvette, France*

[3]*Laser Physics and Nonlinear Optics Group, MESA$^+$ Institute for Nanotechnology, University of Twente, 7500 AE Enschede, The Netherlands*

(Received 2 April 2008; published 10 October 2008)

Recent significant improvements of the contrast ratio of chirped pulse amplified pulses allows us to extend the applicability domain of laser accelerated protons to very thin targets. In this framework, we propose an analytical model particularly suitable to reproducing ion laser acceleration experiments using high intensity and ultrahigh contrast pulses. The model is based on a self-consistent solution of the Poisson equation using an adiabatic approximation for laser generated fast electrons which allows one to find the target thickness maximizing the maximum proton (and ion) energies and population as a function of the laser parameters. Model furnished values show a good agreement with experimental data and 2D particle-in-cell simulation results.

DOI: 10.1103/PhysRevLett.101.155002 PACS numbers: 52.38.Kd, 52.50.Jm, 52.65.Rr, 52.70.Nc

Most of the present or foreseen applications involving laser accelerated ions and/or protons (fast ignition [1], induction of nuclear phenomena [2], isotopes production for medical applications [3], or proton therapy [4], for instance) require copious amounts of high energy charged particles. Recently, it has been experimentally shown that it is possible to increase the maximal ion energy using ultrathin foils irradiated by short ultrahigh contrast (UHC) laser pulses [5,6]. In the first theoretical paper on this item [7], numerical simulations suggested that the optimal foil thickness (ℓ^{opt}) to maximize fast Al ions energy is close to 50 nm for a laser intensity about 10^{19} W/cm^2. Accurate subsequent simulations [8] at 1 order of magnitude higher laser intensity found $\ell^{\mathrm{opt}} \approx 1$ μm. Under appropriate assumptions, the scaling formulas from [9,10] can explain such dependence from thickness for thick foils. A more detailed analysis was done in [11] by several simulations of two layer foils irradiated by a few hundred femtosecond laser pulse with an intensity greater than 10^{19} W/cm^2. According to the deduced scaling formula, ℓ^{opt} is inversely proportional to the plasma density and directly proportional to the square root of the laser intensity.

In this Letter we present an analytical model of ion acceleration using thin foils, based on a self-consistent solution of the Poisson equation for the electric field responsible for ion acceleration and the equation of ion front motion, which describes the target expansion. This model allows us to find ℓ^{opt} for given UHC laser pulse parameters and shows that, decreasing the foil thickness, the maximal ion energy as well as the number of accelerated ions increase. Our model, calibrated with the help of numerical simulations, presents a number of substantial improvements compared with existing ones. Grysmayer and Mora [12] already used the above-mentioned system of equations but they solved it only numerically and for targets with just one kind of ion. Our model is more realistic than the solution of the Poisson equation with a constant ion profile and solves the ion equation of motion in a determined field. Contrary to [13], fast electrons are described using an adiabatic instead of isothermal approximation because the main stage of ion acceleration in the expanding plasma usually begins after the end of the laser pulse. The quasineutral and automodel approximations used in [14–16] are not well fitted to describe the interaction of UHC short laser pulses with the target as in this regime the gradient scale lengths are smaller than the Debye radius of hot electrons (r_{De}). Finally, in the model described in [17], the Poisson equation and the equation of heavy ions movement are solved together, allowing the size of the target to vary with respect to r_{De}. We have carried out a more detailed study of the shape and position of the energy maximum for both light and heavy ions as a function of the target thickness. Unlike [17], we have taken into account the influence of the target thickness onto the laser radiation absorption coefficient and the fast electrons temperature, as well as the mutual influence of light and heavy ion components in the acceleration process. This allowed us to correctly interpret the results of numerical simulations and experiments.

Actually, our model applies to laser intensities ranging from 10^{18} to 10^{20} W/cm^2, for short (<100 fs) and UHC laser pulses. Nonetheless, for the higher considered laser intensities, we observed the appearing of an asymmetry of ions acceleration from the two target opposite sides, the acceleration of the overall target along the direction of the laser pulse, and a spatial separation of the light and heavy ions layers exceeding r_{De}. As a consequence the model needs to be lightly modified to correctly reproduce the interactions at laser intensities $\geq 10^{20}$ W/cm^2: this modification will be the object of a separate following paper.

We employed a 2D PIC code that includes two ion species [18] to get a detailed picture of the acceleration. The average ionization state of carbon ($Z \approx 4$) was calculated using the ADK model [19] of tunnel ionization. As in the UHC ideal case the foil keeps its initial rectangular density shape until the arrival of the main pulse, in the model the laser pulse interacts with a rectangular plasma profile whose ion density is $n_{i0} = 6 \times 10^{22}$ cm^{-3}. We took the hydrocarbon contamination into account by adding an ultrathin hydrogen layer on both target surfaces. We considered 1000, 100, and 50 nm carbon target thickness with a hydrogen contamination layer of 30, 10, and 6 nm, respectively. The other parameters put in the simulation were as follows: $\lambda_L = 0.8$ μm, $I_L = 10^{19}$ W/cm^2, $t_L =$ 65 fs, p polarization and 45° incidence where λ_L, I_L, and t_L are the laser pulse wavelength, intensity, and duration, respectively. The simulations show that ions are accelerated during 150–200 fs and at the end of the calculations (300–400 fs) the distribution function is practically steady. All along the duration of the laser pulse the electron cloud expands to a thickness significantly higher compared with the ion core and larger than the laser spot size in the transverse direction. Target ions get most energy after the end of the laser pulse (>100 fs) when fast electrons have created a steady distribution around the ion core. Because of electron recirculation [20] front and back ion acceleration are almost the same and after the end of the laser pulse there is a quasisymmetrical distribution of particles and fields. The spatial distribution of accelerating electric fields at 100 fs shows the standard shape of symmetrical ''triangles'' close to the ion core [21]. Later on, the maximal field amplitude decreases and the ''triangles'' move out from the initial core as ions begin to expand. The acceleration continues until 150–200 fs for all thicknesses and all along this period electrons show a high temperature. Later on the electrons begin to adiabatically cool down and ions stop to gain energy. As the electron and ion distribution functions at this time are quite similar (Fig. 1) and their spatial distributions have almost the same shape (insets in Fig. 1) we can suppose a quasineutral expansion of the hot plasma cloud. Moreover, ions are accelerated at the normal of the target surface with a quite narrow angular distribution and show an almost symmetrical distribution at foil front and rear.

According to the more qualitative aspects of code results (the symmetry of the plasma expansion, the shape of the accelerating electric field and the duration of the acceleration process) we suggest the following 1D analytical model to calculate the expansion of a thin foil interacting with an UHC laser pulse. A thin foil is located along the y axis and expands under the pressure of fast electrons along the z axis. As ion acceleration continues after the end of the laser pulse we use a 1D adiabatic model of electron gas expansion with the constant $\gamma = 3$. We describe the heavy ion density distribution by a rectangular shape of varying width whereas the hydrogen density distribution on the target surface is modeled by a δ function. The ion acceleration is governed by the Poisson equation for the electric field and the equation of motion of the heavy ion front while the equation of motion of light ion front motion is similar to [13] where the isothermal case was considered. The fast electron density is determined from hydroequations of motion by neglecting the electron mass: $n_e(\varphi) = n_{e_0}(1 + \frac{\gamma-1}{\gamma}\varphi)^{1/(\gamma-1)}$ where n_{e_0} is the initial density of fast electron, $\varphi = |e|\phi/T_{e_0}$ is the normalized potential, and T_{e_0} the initial temperature of fast electrons. This leads to a Poisson equation of the following form:

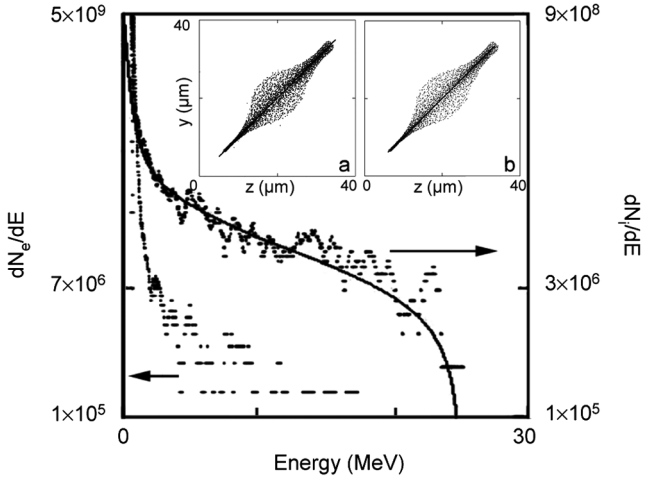

FIG. 1. Electron and carbon ion distribution functions at $t =$ 200 fs for a 60 nm thickness foil. Insets: distribution of electron (a) and ion (b) densities at $t = 400$ fs.

$$\frac{d^2\varphi}{d\xi^2} = \left(1 + \frac{2}{3}\varphi\right)^{1/2} - \frac{N}{b}\theta(b - \xi) - \sigma\delta(\xi - b). \quad (1)$$

Here $\xi = z/r_{\mathrm{De}}$, $r_{\mathrm{De}}^2 = T_{e_0}/4\pi e^2 n_{e_0}$, $\sigma = Z_1 n_{i_1}\ell_{i_1}/n_{e_0}r_{\mathrm{De}}$, $N = Z_2 n_{i_2}\ell_{i_2}/2n_{e_0}r_{\mathrm{De}}$, θ is the unit step function, n_{i_j} and ℓ_{i_j} are, respectively, the ion density and layer thickness ($j = 1$ for hydrogen, 2 for heavy ions) and $b = b(t)/r_{\mathrm{De}}$ is the normalized distance of the ion front. The potential is vanishing at infinity, which ensures the conservation of the electron number, and, due to the symmetry of the plasma slab, is zero field valued at $\xi = 0$. The Poisson equation (1) can be solved analytically:

$$\tilde{\varphi}(\xi) = \frac{1}{4 \times 3^4}[b - \xi + (4 \times 3^4\tilde{\varphi}(b))^{1/4}]^4 \quad \xi \geq b,$$
$$b - \xi(\tilde{\varphi}) = \int_{\tilde{\varphi}(b)}^{\tilde{\varphi}} \frac{d\tilde{\varphi}}{\sqrt{\frac{8}{9}(\tilde{\varphi}^{3/2} - \tilde{\varphi}(0)^{3/2}) - \frac{4N}{3b}(\tilde{\varphi} - \tilde{\varphi}(0))}}$$
$$0 \leq \xi \leq b, \quad (2)$$

where $\tilde{\varphi} = (1 + (2/3)\varphi)$. The integration constants for $b \gg 1$, $N > 1$, and $\sigma < 1$ are

$$\tilde{\varphi}(0) \approx (N/b)^2, \qquad \tilde{\varphi}(b) \approx \frac{N^2}{3b^2}\left(1 + \frac{2\sqrt{2}\sigma b^{3/2}}{3^{3/4}N^{3/2}}\right).$$

According to formula (2), the electric fields before (+) and beside (−) the hydrogen layer become $E_\delta^\pm = 2\pi e(Z_2 n_{i_2}\ell_{i_2} \pm Z_1 n_{i_1}\ell_{i_1})$ and $E_\infty^\pm = \sqrt{4\pi Z_2 n_{i_2} T_{e_0}}(\sqrt{2}/3^{3/4})(Z_2 n_{i_2}/n_{e_0}) \pm 2\pi e Z_1 n_{i_1}\ell_{i_1}$, respectively, for very thin ($b \ll 1$) and thick ($b \gg 1$) targets. The equations of motion of light and heavy ion fronts under the action of the electric field are consequently

$$m_{i_{1,2}}\frac{\partial^2 b_{1,2}}{\partial t^2} = Z_{1,2}e\left(\frac{E_\delta^\pm}{\sqrt{1+(\ell_{i_2}/r_{\mathrm{De}})^2}}\frac{1}{1+(b_{1,2}/r_{\mathrm{De}})^{3/2}} + \frac{E_\infty^\pm}{\sqrt{1+(r_{\mathrm{De}}/\ell_{i_2})^2}}\frac{1}{1+(b_{1,2}/r_{\mathrm{De}})^{3/2}}\right). \quad (3)$$

Here $b_{1,2}$ are the coordinates of light and heavy ion fronts. Using Eq. (1) to describe the electric fields of the two ion fronts is correct only if $|b_1 - b_2| < r_{\mathrm{De}}$. This inequality is verified at the main stage of the acceleration because in the opposite case each ion front is surrounded by its own Debye screen and interaction between them is stopped. The initial conditions of Eq. (3) are ($\ell_{i_1} \ll \ell_{i_2}$):

$$\left.\frac{\partial b_{1,2}}{\partial t}\right|_{t=0} = 0, \qquad b_{1,2}|_{t=0} = \frac{\ell_{i_2}}{2}. \quad (4)$$

The energy conservation law for Eq. (3) allows us to give the following expression for ion energies: $\varepsilon_{i_{1,2}} = (m_{i_{1,2}}/2)(\partial b_{1,2}/\partial t)^2$. As a consequence, for $b \to \infty$:

$$\varepsilon_{i\mathrm{max}_{1,2}} \approx \frac{2.4 Z_{1,2} e E_\delta^\pm r_{\mathrm{De}}}{\sqrt{1+(\ell_{i_2}/r_{\mathrm{De}})^2}} + \frac{2 Z_{1,2} e E_\infty^\pm r_{\mathrm{De}}}{\sqrt{1+(r_{\mathrm{De}}/\ell_{i_2})^2}}. \quad (5)$$

We estimate the fast electron temperature for an ultrathin foil from the following formula:

$$T_{e_0}(\ell_{i_2}) \approx \frac{\eta(\ell_{i_2}) I_L t_L}{Z n_{i2}\ell_{i_2}}, \quad (6)$$

where $\eta(\ell_{i_2})$ is the absorption coefficient for a ℓ_{i_2} thickness target. One has to note that the value of the electron temperature for $\ell_{i_2} \to \infty$ in Eq. (6) is given by the ponderomotive potential [22] $T_{e0}|_{\ell_{i_2}\to\infty} = m_e c^2(\sqrt{1 + I_L\lambda_L^2/1.37\times 10^{18}\ \mathrm{W/cm^2}} - 1)$. We then used again the PIC code to deduce the foil thickness dependence of the absorption coefficient:

$$\eta(\ell_{i_2}) \approx \frac{\eta_\infty \ln(1+\ell_{i_2}/L_{\mathrm{trans}})}{1+\ln(1+\ell_{i_2}/L_{\mathrm{trans}})}. \quad (7)$$

Here the transparency length $L_{\mathrm{trans}} \approx \ell_s$ where ℓ_s is the skin depth whereas $\eta_\infty \approx 0.5$ is the absorption coefficient of a bulk target. We suppose that the density of fast electrons is close to the initial plasma density because laser light penetrates deep into an ultrathin foil and ionize it instantly: $n_{e0} \approx Z_2 n_{i_2} f(\ell_{i_2})$ where $f(\ell_{i_2}) \sim 1$. Finally, inserting formulas (6) and (7) into (5) we obtain the expression of maximal ion energy:

$$\varepsilon_{i\mathrm{max}_{1,2}} \approx \frac{3\pi Z_{1,2} e^2 (Z_2 n_{i_2}\ell_{i_2} \pm Z_1 n_{i_1}\ell_{i_1}) r_{\mathrm{De}}}{\sqrt{1+(\ell_{i_2}/r_{\mathrm{De}})^2}} + (0.34 \pm 4\pi e^2 Z_1 n_{i_1}\ell_{i_1} r_{\mathrm{De}})\frac{Z_{1,2}}{\sqrt{1+(r_{\mathrm{De}}/\ell_{i_2})^2}} \quad (8)$$

Supposing a low number of light ions compared with heavy ones, the foil thickness which optimizes the ion energy (8) is given by

$$\ell_{i_2}^{\mathrm{opt}} \approx \lambda_L \frac{n_{\mathrm{cr}}}{Z n_{i_2}}\left(5 + I_{18}^{3/4}\left(\frac{t_L}{30\,\mathrm{fs}}\right)^{3/4}\right)(0.1 Z n_{i2}/n_{i0})^{-1/2}, \quad (9)$$

where $n_{\mathrm{cr}} = \sqrt{4\pi n_e e^2/m_e}$ is the plasma critical density and $I_{18} = I_L/10^{18}\ \mathrm{W/cm^2}$. As mentioned above, at long times the plasma reaches a quasineutral spatial distribution (see insets in Fig. 1). We can therefore use the quasineutral condition and solve the set of hydroequations under the adiabatic approximation. As a consequence the ion distribution function is

$$\frac{\partial N_j}{\partial \varepsilon} \approx \frac{2N_j}{\pi\sqrt{\varepsilon_{i\mathbf{max}_j}\varepsilon}}\left(1 - \frac{\varepsilon}{\varepsilon_{i\mathbf{max}_j}}\right)^{1/2}.$$

This dependence is very close to the shape of the simulated distribution function (see Fig. 1).

Finally we checked the effectiveness of our model obtaining a close agreement with the measurements obtained in an UHC laser ion acceleration experiment and with PIC code results. The experiment was performed at the Saclay Laser Interaction Center Facility, using the UHI10 Ti-sapphire laser delivering 10 TW ultrashort pulses (65 fs). The intrinsic 10^6 contrast of the beam was raised to 10^{10} thanks to a "double plasma mirror" [23]. The laser beam was focused to a spot size of 8 μm (FWHM) under 45° incidence angle and p polarization, on thin Mylar foils with thicknesses varying between 0.1 and 10 μm and carbon foils from 80 to 25 nm. The laser intensity was $10^{18}\ \mathrm{W/cm^2}$. Proton spectra were simultaneously recorded using two similar Thomson parabola placed normally to the target in the laser direction (FWD) and opposite to laser direction (BWD). For foils thinner than 0.1 μm, due to a different setup, we recorded the BWD emission only. We found a maximal FWD C^{4+} ion and proton energy at about 3.5 and 2 MeV, respectively, and an optimal foil thickness at about 100 nm. Experimental maximum proton and C^{4+} energies and variation of particles number (in relative units) as a function of the target thickness are shown in Figs. 2(a) and 2(b). The values given by our model are in quite good agreement both with the PIC code and experimental results.

We used our model to estimate the number of ions moving out from the foil too. Because of the exponential decrease of the electric field inside the target ($z < 0$), an ion at the initial position $z_0 < 0$ gets an energy $\varepsilon_{i_{1,2}}(z_0) \approx \varepsilon_{i\mathbf{max}_{1,2}} e^{z_0/\ell_s}$. Supposing to collect only ions with an energy higher than a given detector energy threshold ($\varepsilon_{\mathrm{thr}}$)

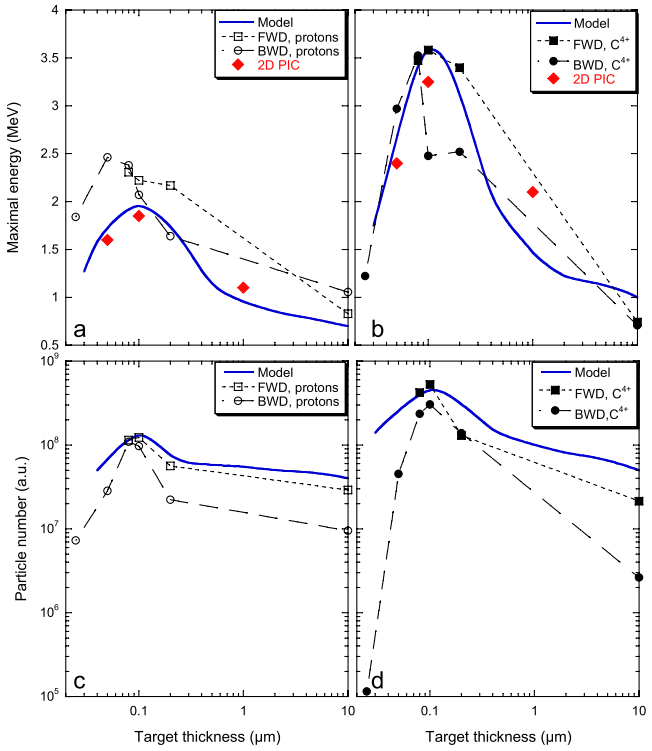

FIG. 2 (color online). Maximal experimental energies and number of particles for protons [(a) and (c)] and carbon ions [(b) and (d)] as a function of foil thickness. Open and closed black circles and squares are experimental data. The solid blue lines are the analytical model estimations. Closed red diamonds are 2D PIC code results.

the total number of ions (N_H, N_C—protons, carbon ions) on the detector can be estimated using

$$\begin{aligned} N_H &= \int_{-\infty}^{-\ell_H} n_{HC}\theta(\varepsilon_{i_1}(z_0) - \varepsilon_{th})dz_0 \\ &\quad + \int_{-\ell_H}^{0} n_H\theta(\varepsilon_{i_1}(z_0) - \varepsilon_{th})dz_0 \\ &= n_{HC}\ell_1\theta(\ell_1/r_{\mathrm{De}}) + n_H\ell_H\theta(\ell_1/r_{\mathrm{De}}) \\ &\quad + n_H\ell_S\theta(-\ell_1/r_{\mathrm{De}}), \\ N_C &= \int_{-\infty}^{-\ell_H} n_C\theta(\varepsilon_{i_2}(z_0) - \varepsilon_{th})dz_0 = n_C\ell_2\theta(\ell_2/r_{\mathrm{De}}), \end{aligned} \tag{10}$$

where $\ell_{1,2} = \ell_S \ln(\varepsilon_{i\max_{1,2}}/\varepsilon_{\mathrm{th}}) - \ell_H$ and n_{HC} and n_H are the density of hydrogen inside the foil and on the surface layer, respectively. The dependence of ions number on foil thickness is included in $\varepsilon_{i\mathbf{max}}$ and therefore in $\varepsilon(z_0)$. The constants $n_{C,H}$ are properly chosen to fit the experimental and simulated maximum values. The results, showing a good agreement with experimental data, are presented in Figs. 2(c) and 2(d). Once again a foil thickness of about 100 nm maximizes the particle number for both ion kinds.

In conclusion, we have presented an analytical model, to be used in the framework of UHC laser ion acceleration, which correctly describes the variation of maximum ion energies and population as a function of the target thickness. It appears that an optimized thickness, depending on laser parameters and target density, can increase the accelerated ion energy and population. We have shown that ion acceleration in a thin target continues after the end of the laser pulse almost symmetrically from both foil sides and drops down after the adiabatic cooling of fast electrons. Finally, we have checked the effectiveness of our model obtaining a close agreement with the results of an experiment using UHC pulses on ultrathin targets.

This work was partly supported by the Conseil Général de l'Essonne (ASTRE program) and the ECO-NET program. One of us (R. L.) thanks the Dutch Ministry of Education, Culture and Science (OC & W) for support.

[1] M. Tabak *et al.*, Phys. Plasmas **1**, 1626 (1994).
[2] K. W. D. Ledingham *et al.*, Science **300**, 1107 (2003).
[3] I. Spencer *et al.*, Nucl. Instrum. Methods Phys. Res., Sect. B **183**, 449 (2001).
[4] S. S. Bulanov *et al.*, Med. Phys. **35**, 1770 (2008).
[5] D. Neely *et al.*, Appl. Phys. Lett. **89**, 021502 (2006).
[6] T. Ceccotti *et al.*, Phys. Rev. Lett. **99**, 185002 (2007).
[7] Q. L. Dong, Z.-M. Sheng, M. Y. Yu, and J. Zhang, Phys. Rev. E **68**, 026408 (2003).
[8] E. D'Humières *et al.*, Phys. Plasmas **12**, 062704 (2005).
[9] Y. Oishi *et al.*, Phys. Plasmas **12**, 073102 (2005).
[10] J. Fuchs *et al.*, Nature Phys. **2**, 48 (2006).
[11] T. Esirkepov, M. Yamagiwa, and T. Tajima, Phys. Rev. Lett. **96**, 105001 (2006).
[12] T. Grismayer and P. Mora, Phys. Plasmas **13**, 032103 (2006).
[13] B. J. Albright *et al.*, Phys. Rev. Lett. **97**, 115002 (2006).
[14] P. Mora, Phys. Rev. Lett. **90**, 185002 (2003).
[15] P. Mora, Phys. Rev. E **72**, 056401 (2005).
[16] J. Schreiber *et al.*, Phys. Rev. Lett. **97**, 045005 (2006).
[17] M. Murakami and M. M. Basko, Phys. Plasmas **13**, 012105 (2006).
[18] A. J. Kemp and H. Ruhl, Phys. Plasmas **12**, 033105 (2005).
[19] M. Ammosov *et al.*, Sov. Phys. JETP **64**, 1191 (1986).
[20] Y. Sentoku *et al.*, Phys. Plasmas **10**, 2009 (2003).
[21] M. Passoni, V. T. Tikhonchuk, M. Lontano, and V. Y. Bychenkov, Phys. Rev. E **69**, 026411 (2004).
[22] S. C. Wilks *et al.*, Phys. Plasmas **8**, 542 (2001).
[23] A. Lévy *et al.*, Opt. Lett. **32**, 310 (2007).